

# Modelling and simulation of D-class current-fed parallel resonant inverter for induction heating system

Leyla Arslan<sup>1</sup>, Harun Özbay<sup>2</sup>

<sup>1</sup>Department of Electrical-Electronics Engineering Bandırma Onyedi Eylül University, Bandırma, Turkey  
leylaarslan@ogr.bandirma.edu.tr, ORCID: 0000-0001-6326-6269

<sup>2</sup>Department of Electrical Engineering, Bandırma Onyedi Eylül University, Bandırma, Turkey, hozbay@bandirma.edu.tr,  
ORCID: 0000-0003-1068-244X

In the induction heating process, non-contact heating is carried out. Induction heating systems are used in heating, melting, surface hardening processes and applications such as cooking. Induction heating is based on Michael Faraday's Law of Induction. Compared to conventional heating methods, the induction heating method has advantages such as shorter processing time, uniform distribution of heat on the material, high efficiency and no explosion hazard. In order to realize induction heating, a variable magnetic field and a metal material placed in the magnetic field are needed. Voltage-fed or current-fed resonant inverters are frequently used to realize power conversion in induction heating and because of their low switching losses and zero current or voltage switching possibilities. In this study, D-class current-fed parallel resonant inverter, which is one of the resonant converter types, is used. The operating states of the switching frequency below the resonant frequency, equal to the resonant frequency, and above the resonant frequency have compared. The simulation results were obtained by modeling the designed current source parallel resonance inverter with PSIM software. Thus, it has been observed that the phase difference between the output current and voltage in the parallel resonant inverter depends on the switching frequency. As a result of the operation of the resonant inverter at the resonant frequency, it has been determined that zero voltage switching is provided. Thus, it has been observed that maximum efficiency is achieved by preventing switching losses and the obtained results are presented.

**Keywords:** Induction Heating Systems, Parallel Resonance Inverters, PSIM

© 2022 Published by AInteliala

## 1. Introduction

The basis of induction heating is based on the principle of inducing voltage when a conductive material is placed in a time-varying magnetic field, which is considered an important development in electromagnetic theory and was discovered by Michael Faraday in 1831 [1]. This induced voltage causes electron flow, that is, current. These currents are called Eddy currents. When Eddy currents pass through the conductive material, a resistance occurs against the movement of electrons. This resistance emerges as heat and the principle of induction heating occurs. Induction heating systems are systems that convert electrical energy into heat energy. Its advantages compared to other heating systems are that the heating process is short-lived, the heat is distributed homogeneously on the metal material, high efficiency and there is no danger of explosion [2].

A. Polsripim et al., in their study, suggested the use of class D current source resonance inverter for induction heating system with ferromagnetic load. When the load parameters change, the resonant frequency increases. The inverter operates in the range of 90.5-92.6 kHz depending on the load condition. When the load parameters change, the phase angle can be changed to keep the operating frequency higher than the natural frequency and maximum power is transferred to the load during heating. For future work, they concluded that the existing sensor of the induction coil could be used to send a control signal to a PFC converter to accurately control the power by adjusting the duty cycle of the switch [3].

A. Suresh and S. R. Reddy proposed modeling a closed-loop controlled class D current source resonance inverter for ferromagnetic load. In the study, they aimed to develop an induction heater system with minimum equipment. Simulink model of closed loop system and simulation results are presented. It has been observed that the closed-loop system can maintain a constant voltage. They concluded that this system has the advantages of reduced volume and reduced hardware [4].

J. Jittakort et al. proposed the use of a class D current source resonant inverter with an interspersed buck converter for a non-ferromagnetic loaded induction heating system. The maximum output power transferred to the load for the hardware prototype is 1.26 kW. The resonant inverter operates with a fixed frequency of 108 kHz, while the buck converter operates at 40 kHz for soft switching operation. It has been concluded that the non-ferromagnetic workpiece can be used because the inverter operates at a fixed switching frequency and the effect of parameter change is minimal under increasing temperature [5].

C. Ekkaravarodome et al. presented the design method of class D current source resonance inverter for an induction cooker with zero fluctuating line current in their study. The design procedure is based on the principle of class D current source resonant inverter with a simplified load network model, which is a parallel equivalent circuit. A laboratory prototype of 2500 W for 220 V<sub>rms</sub>/50 Hz mains line was developed to theoretically validate the analysis. Finally, they concluded that the zero-ripple line current class D current source resonant inverter for use in household induction cookers with parallel resonance equivalent circuits has a power factor close to 1, a THD of 4.7%, and an efficiency of 96.26% [6].

In order to carry out the heating process in induction heating applications, a high frequency alternating voltage must be obtained at the output from the energy taken from the input source. For this, the alternating voltage provided by the input source must first be converted to direct voltage with a rectifier, and then converted to an alternating voltage with the desired amplitude and frequency at the output with an inverter.

Resonance topology is used to convert the direct voltage at the rectifier output to alternating voltage with minimum loss and to reduce the switching losses in the inverter circuits. In resonant converter circuits, higher output power occurs at the resonant frequency and the efficiency increases. For this reason, the use of resonant circuits is preferred in induction heating applications [7].

Resonant converters are basically divided into two main groups as series and parallel, and each of them is divided into different subgroups within itself. In the series resonance circuit, the resistors, inductors and capacitors connected in series are fed by the voltage source, while in the parallel resonance circuit, the same elements connected in parallel are fed by the current source. A sufficiently large coil ( $L_{dc}$ ) connected to the input voltage source can be referred to as a current source [8].

One of the biggest advantages of a current source parallel resonant inverter is that there is no need for an isolated drive circuit as both switches are connected to ground. Figure 1. shows the D-class current fed parallel resonant inverter circuit.

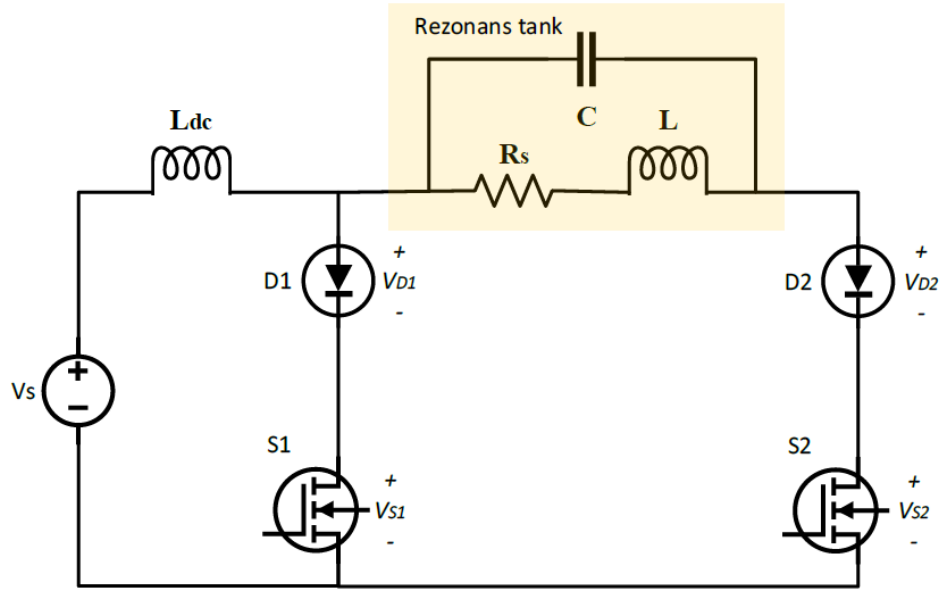


**Figure 1.** Class D current fed parallel resonant inverter circuit

In a typical voltage source series resonant inverter, the inverter output voltage increases as the switching frequency approaches the resonant frequency. In a current source parallel resonance inverter, on the other hand, the output voltage decreases as the switching frequency approaches the resonant frequency.

The circuit requires unidirectional switches for current and bidirectional switches for voltage. Each switch consists of a MOSFET in series with a diode. Thus, the switch can only conduct a positive current and block either positive or negative voltage.

The resistance  $R_s$  in series with the resonant coil  $L$  is calculated as the parallel resistance  $R_p$  by providing the impedance conversion with equation (1). In this case, the equivalent circuit will be as given in Figure 2.

$$Z = \sqrt{R_s^2 + (\omega L)^2} = \sqrt{R_s^2 + X_L^2} \Rightarrow R_p = \frac{Z^2}{R_s} \quad (1)$$

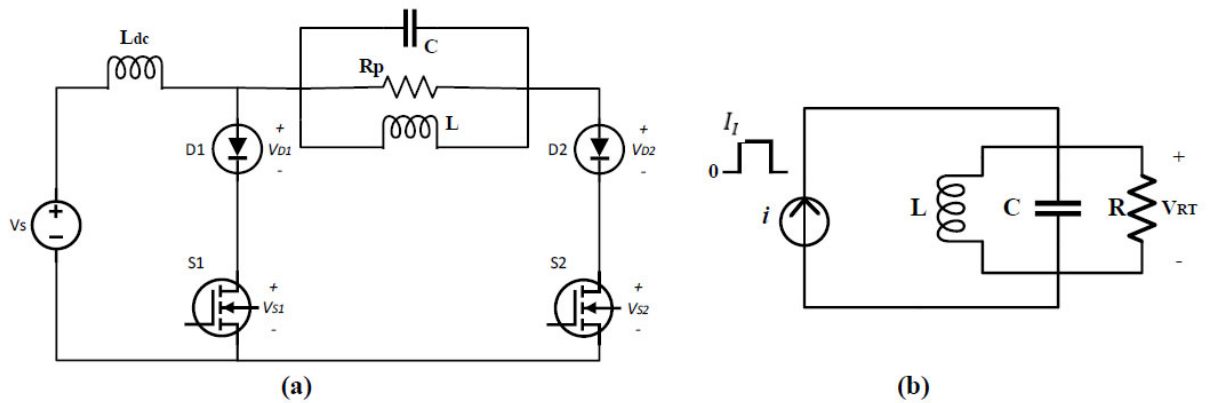


**Figure 2.** a) Current fed parallel resonance inverter circuit with series-parallel impedance conversion, b) Current fed parallel resonant inverter equivalent circuit

## 2. Circuit Analysis

MOSFETs are driven with signals  $V_{GS1}$  and  $V_{GS2}$  at an operating frequency of  $f = 1/T$  and a duty cycle of slightly greater than 50%. To ensure continuity of the input current ( $I_{Ldc}$ ) in the circuit, one or both of the switches must be conducting. Therefore, very short overlapping gate signals must be applied to achieve simultaneous conduction of power MOSFETs.

To determine the value of filter coil  $L_{dc}$  in the circuit, the case where the switching frequency is equal to the resonant frequency is analyzed. The current flowing through the filter coil increases when switch  $S_1$  is turn-on and decreases when switch  $S_2$  is turn-on. When the  $S_1$  switch is turn-on, the voltage on the filter coil is  $V_I$ . In this case, the peak-to-peak value of the ripple current on the filter coil can be expressed by equation (2).

$$I_{Ldc} = \frac{V_I}{L_{dc}} \left( \frac{T}{2} \right) \quad (2)$$

The minimum value of the filter coil for the maximum allowable surge current can be represented by equation (3).

$$L_{dc(min)} = \frac{V_I}{2f_s I_{Ldc(max)}} \quad (3)$$

The parallel resonant circuit consists of a capacitor  $C$ , a coil  $L$  and a resistor  $R$ . The  $R$  resistance is shown in equation (4).

$$R = \frac{1}{G} = \frac{R_p R_d}{R_p + R_d} \quad (4)$$

$R_p$  is the AC load resistance and  $R_d$  is the parasitic resistance of the resonant circuit. Parasitic resistance  $R_d$  can be given by equation (5).

$$R_d = \frac{R_{Lp} R_{Cp}}{R_{Lp} + R_{Cp}} \quad (5)$$

$R_{Lp}$  is the equivalent parallel resistance (EPR) of  $L$  and  $R_{Cp}$  is the EPR of  $C$ . The relationships between ESRs and EPRs are given in equation (6) and equation (7).

$$R_{Lp} = r_L (1 + Q_{L0}^2) \approx r_L Q_{L0}^2 \quad (6)$$

$$R_{Cp} = r_C (1 + Q_{C0}^2) \approx r_C Q_{C0}^2 \quad (7)$$

Here  $Q_{L0} = \omega L / r_L = R_{Lp} / (\omega L)$  and  $Q_{C0} = 1 / (\omega C r_C) = \omega C R_{Cp}$  are the no-load quality factors of  $L$  and  $C$ , respectively.

The characteristic impedance, resonance frequency and quality factor of a current source parallel resonant circuit can be expressed as shown in equation (8), equation (9) and equation (10), respectively.

$$Z_0 = \omega_0 L = \frac{1}{\omega_0 C} = \sqrt{\frac{L}{C}} \quad (8)$$

$$\omega_0 = 2\pi f_0 = \frac{1}{\sqrt{LC}} \quad (9)$$

$$Q_L = \omega_0 C R = \frac{R}{\omega_0 L} = \frac{R}{Z_0} = \frac{1}{G Z_0} \quad (10)$$

The working principle of the current source parallel resonance inverter can also be expressed by the current and voltage waveforms shown in Figure 3.

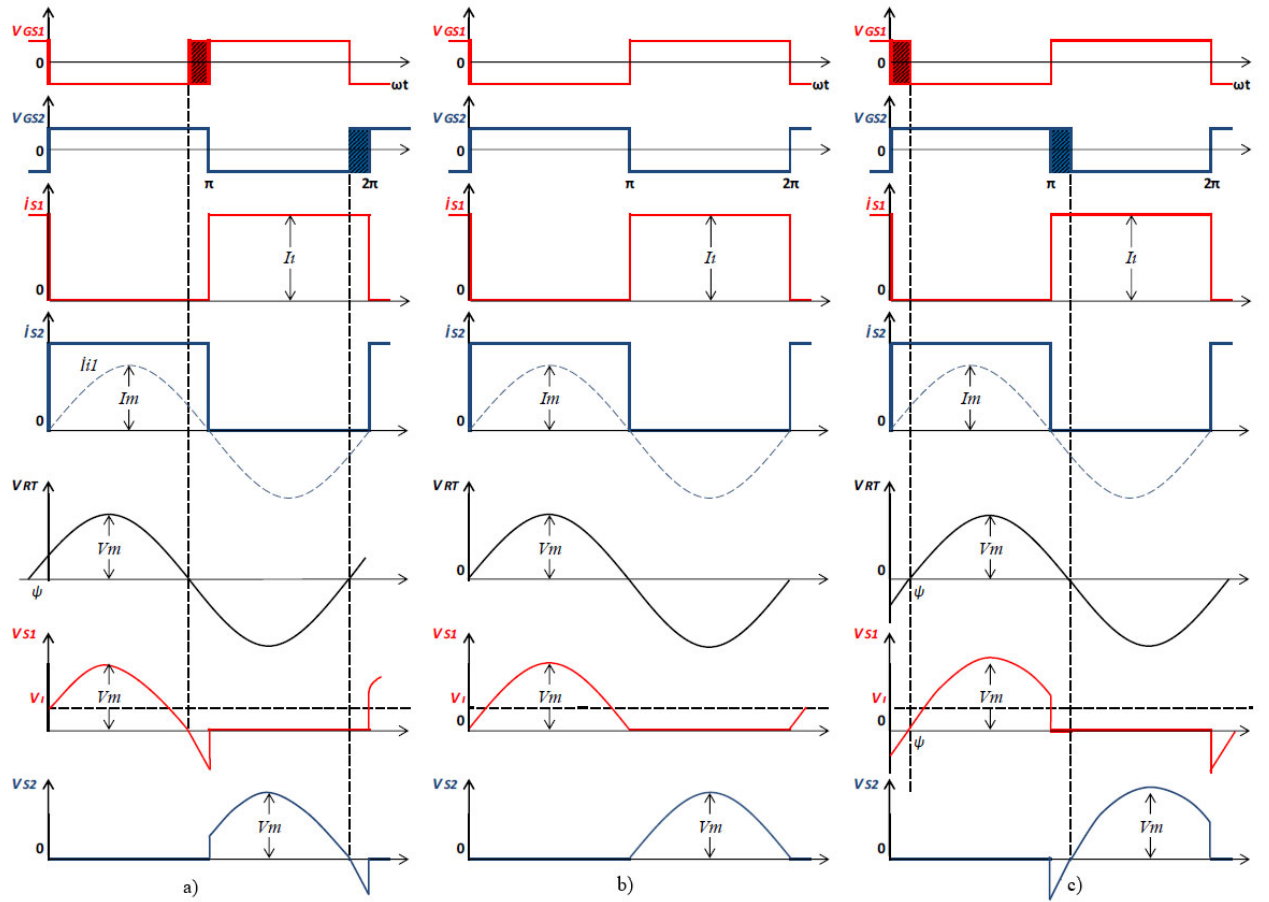


**Figure 3.** Current-voltage waveforms of parallel resonance inverter a)  $f < f_0$ , b)  $f = f_0$ , c)  $f > f_0$

### 3. Simulation Results for Different Switching Frequencies

D-class current fed parallel resonance inverter application, which circuit parameters are given in Table 1., has been implemented in Psim software. The parallel resonance inverter shown in Figure 4. has been analyzed for three different cases and the simulation results are shown. First, the case where the switching frequency is above the resonance frequency ( $f_s = 1.1f_r$ ), then the case where it is equal to the resonance frequency ( $f_s = f_r$ ) and finally the case where it is below the resonance frequency ( $f_s = 0.9f_r$ ) are examined.

**Table 1.** Circuit parameters

Source voltage	$V_s$	48 V
Filter coil	$L_{dc}$	0.62 mH
Resonant coil	$L_{eq}$	3 $\mu$ H
Resonant capacitor	$C_p$	1.5 $\mu$ F
Parallel resistor	$R_p$	28.2 $\Omega$
Resonant frequency	$f_r$	75026.35967 Hz

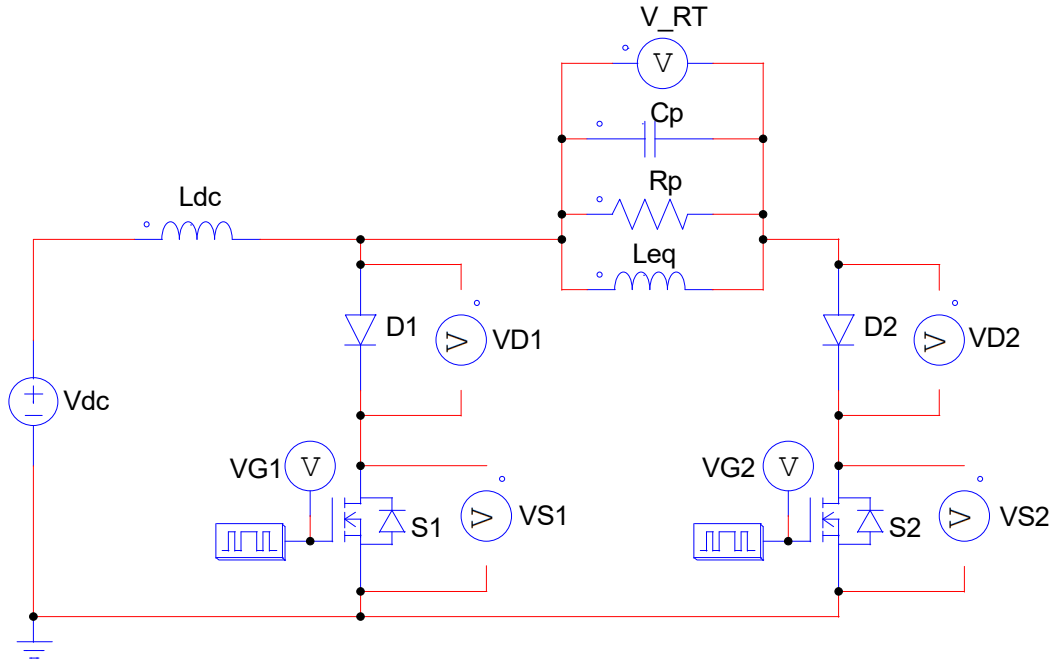


**Figure 4.** Current fed parallel resonance inverter realized in PSIM

#### The case where the switching frequency is above the resonant frequency ( $f_s = 1.1f_r$ )

In the case of  $f_s > f_r$ , the parallel resonant circuit is capacitive. Because of this equivalent capacitance, the amplitude of the load voltage drops and lags behind the current. In mode-1 operating state, both gate signals are in logic 1 state in time interval  $t_0-t_1$  and both switches are in conduction. At  $t=t_0$  moment,  $S_2$  switch turn-on from turn-off and since no current flows through  $S_2$  switch at this moment, zero current (ZCS) conduction condition is achieved.  $S_1$  switch turns-off at zero current and voltage at  $t=t_1$  instant.

Mode-2 operation is realized at time  $t_1-t_2$ . During this time, switch  $S_1$  is in turn-off and switch  $S_2$  is turn-on.  $I_{Ldc}$  the input current flows towards the resonance tank and the energy is transferred to the resonant circuit.

In mode-3 operating state, both gate signals are in logic 1 state in time interval  $t_2-t_3$  and both switches are in conduction. At  $t=t_2$ , switch  $S_1$  switches from turn-off to conduction under ZCS conditions, and at this moment, no current flows from switch  $S_2$  because the diode  $D_2$  is reverse biased. At  $t=t_3$ , switch  $S_2$  is turn-off with zero voltage and zero current.

Mode-4 operating state occurs at time  $t_3-t_4$ . During this time, switch  $S_1$  is turn-on and switch  $S_2$  is in turn-off. The energy stored in the resonance tank is partially discharged to the load and the cycle continues again with Mod-1. Figure 5. and Figure 6. show the simulation results for the  $f_s > f_r$  condition.

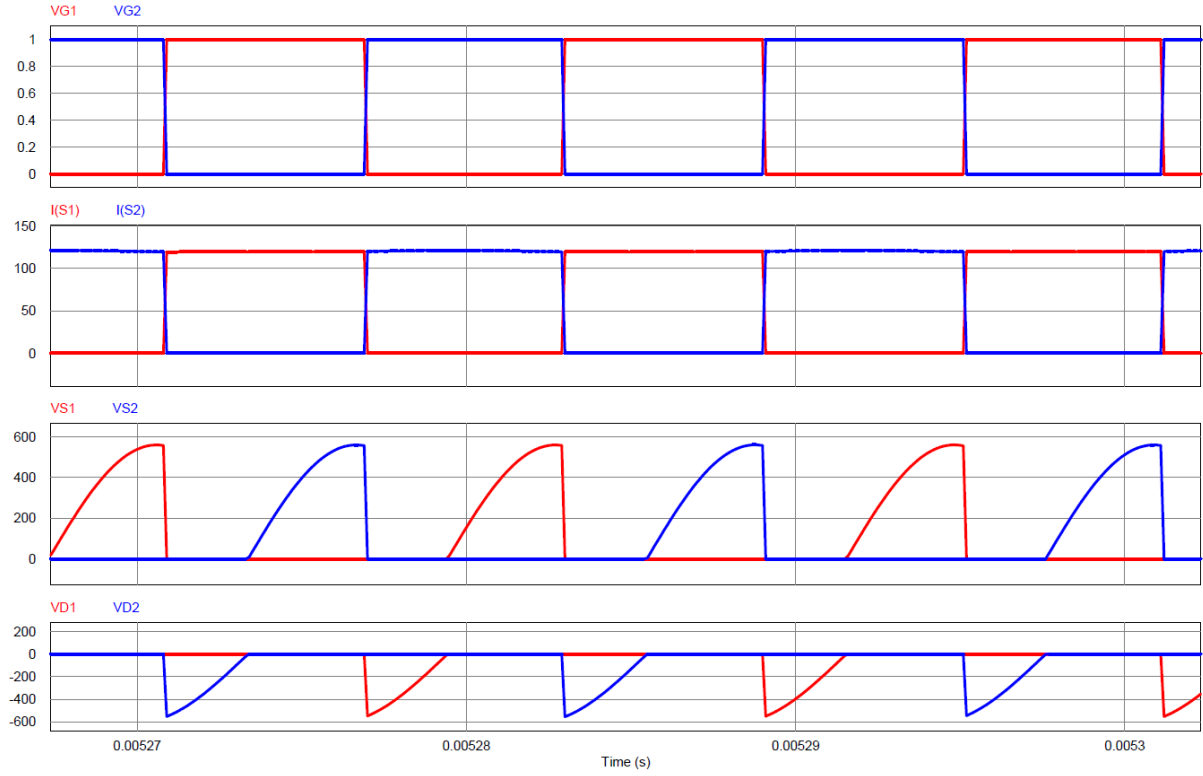


**Figure 5.** Simulation results for the switching condition  $f_s > f_r$

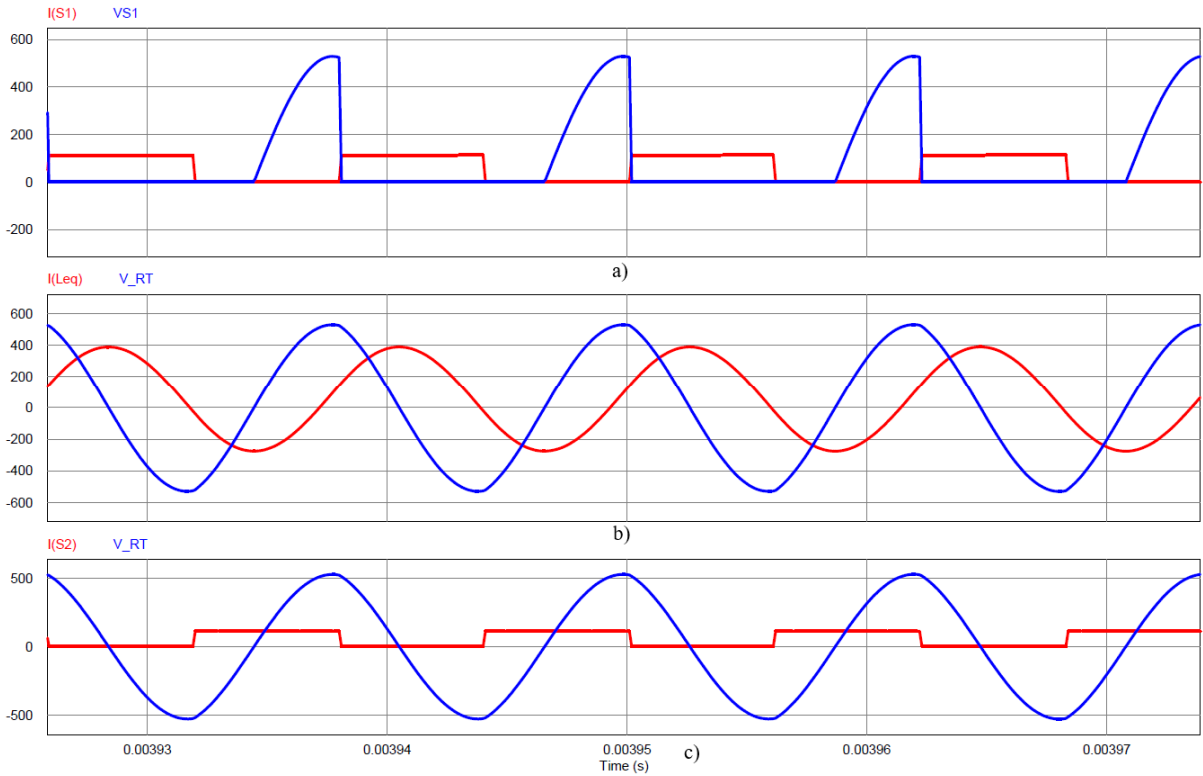


**Figure 6.** For the  $f_s > f_r$  case; a) Current and voltage of switch  $S_1$ , b) Current and voltage of the resonant coil, c) Current of switch  $S_2$  and voltage of resonant coil

### The case where the switching frequency is equal to the resonant frequency ( $f_s=f_r$ )

At the resonant frequency, MOSFETs turn-on and turn-off at zero voltage, which means zero voltage switching, zero switching loss and high efficiency. In this case, since the switch voltages are not negative, series diodes are not required and can be removed, reducing conduction losses. However, when the diodes are deactivated, the output voltage cannot be controlled by changing the frequency. When the switching frequency changes, it does not operate at the resonant frequency and a negative voltage occurs in the switch. Since this voltage cannot be blocked in the absence of a diode, very high currents pass through the switch, causing serious damage to the circuit.

In the case of  $f_s=f_r$ , the inductive impedance  $X_L$  will be equal to the capacitive impedance  $X_C$  and the circuit will have pure ohmic impedance. The voltage of the resonant tank is approximately sinusoidal and in phase with the current. Figure 7. and Figure 8. show the simulation results for the  $f_s=f_r$  condition.

The reverse bias voltages on the power diodes are caused by working very close to full resonance and increase as they move away from resonance.

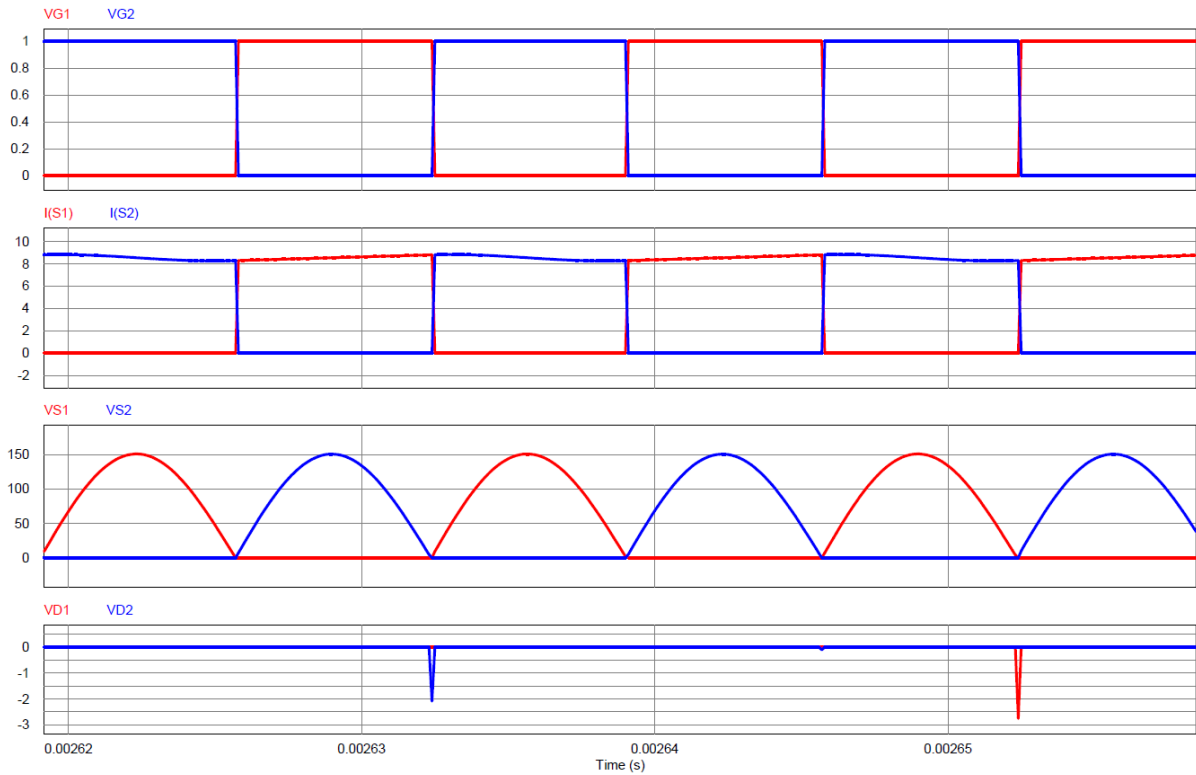


**Figure 7.** Simulation results for the switching condition at the resonant frequency



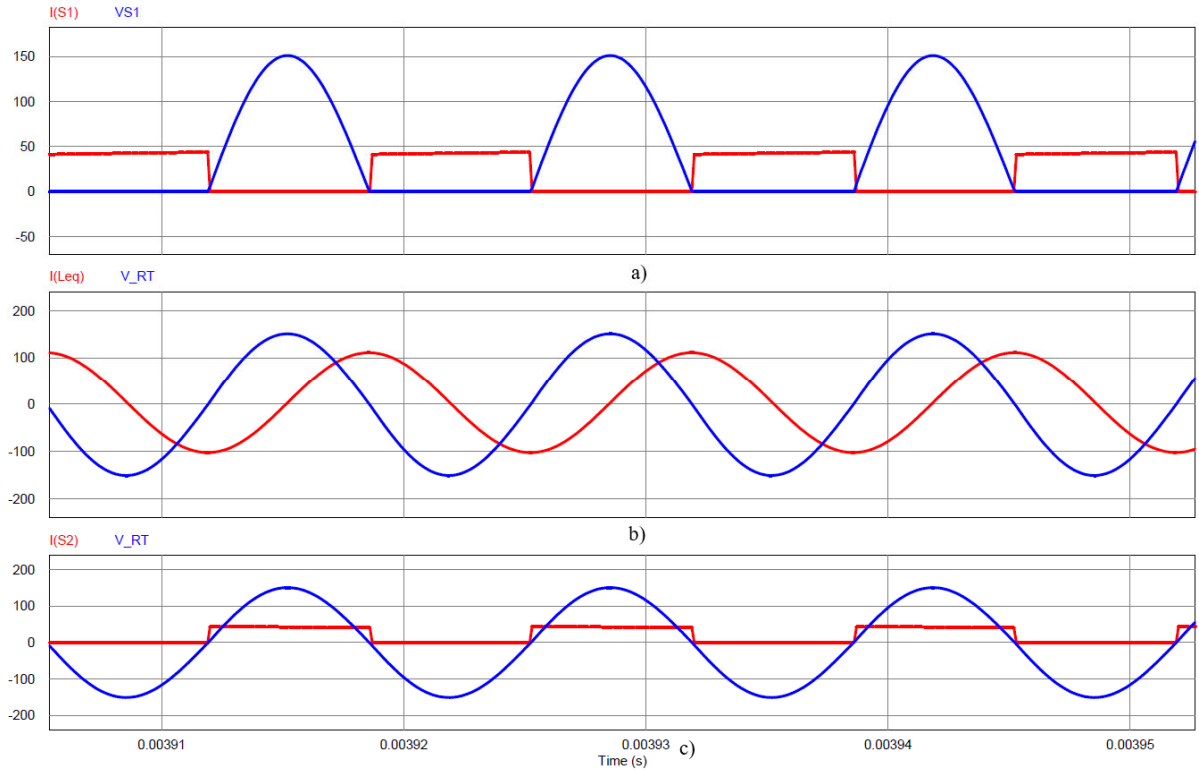


**Figure 8.** For the switching condition at the resonant frequency; a) Current and voltage of switch  $S_1$ , b) Current and voltage of the resonant coil, c) Current of switch  $S_2$  and voltage of resonant coil

#### The case where the switching frequency is below the resonance frequency ( $f_s = 0.9f_r$ )

In the case of  $f_s < f_r$ , the parallel resonant circuit is inductive. Due to the current of this equivalent inductance, the amplitude of the load voltage decreases and is ahead of the current.

If we take into account the mode-1 operating situation, at  $t=t_0$  the switch  $S_2$  turn-on from the turn-off and at this moment the current and voltage of  $S_2$  are zero. At  $t=t_1$ , switch  $S_1$  is turn-off and at this moment, no current is flowing through switch  $S_1$ . Therefore, zero current (ZCS) switching is made.

Mode-2 operation is realized at time  $t_1-t_2$ . During this time, switch  $S_1$  is turn-off and switch  $S_2$  is turn-on.

In mode-3 operating state, both gate signals are in logic 1 state in time interval  $t_2-t_3$  and both switches are in conduction. At  $t=t_2$ , switch  $S_1$  switches from turn-off to conduction with zero voltage and zero current. At  $t=t_3$ , switch  $S_2$  is turn-off at zero current (ZCS).

Mode-4 operating state occurs at time  $t_3-t_4$ . During this time, switch  $S_1$  is turn-on, switch  $S_2$  is turn-off, and the cycle continues with Mode-1 again.

In Figure 9. and Figure 10., simulation results according to switching modes and operating states are shown.

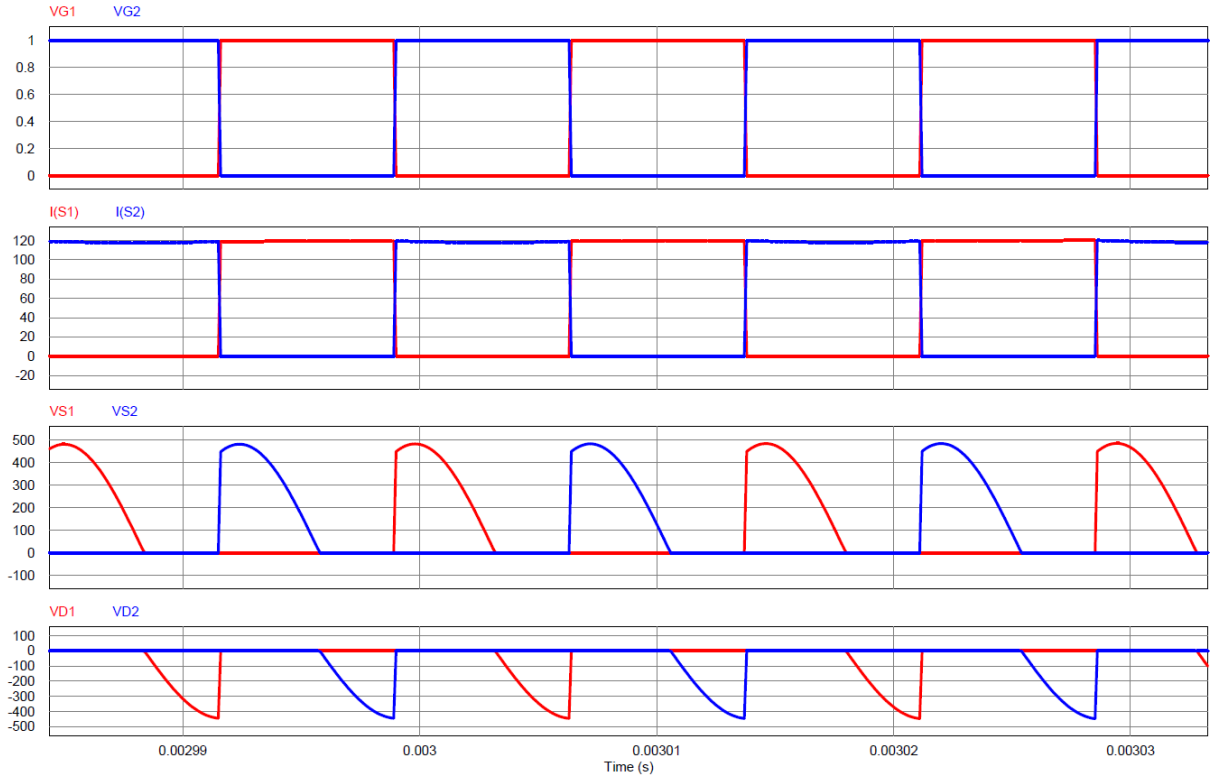


**Figure 9.** Simulation results for  $f_s < f_r$  switching condition

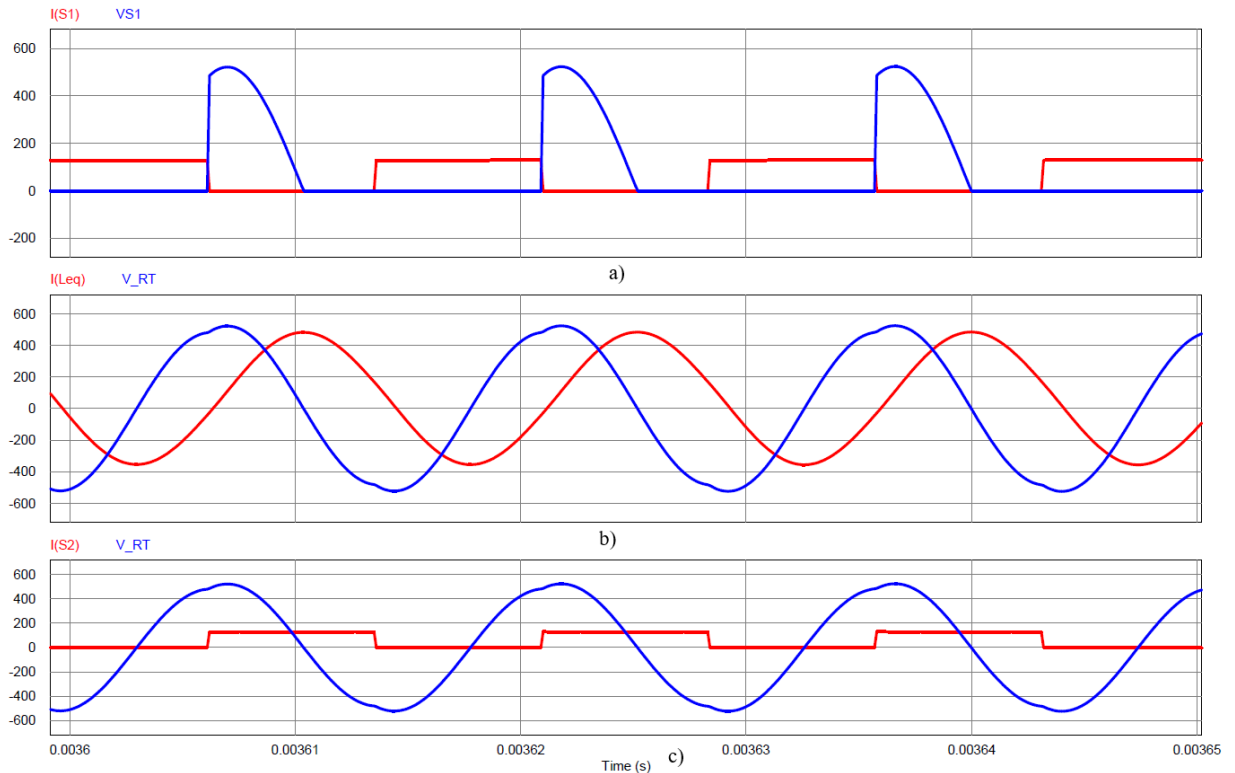


**Figure 10.** For the  $f_s < f_r$  case; a) Current and voltage of switch  $S_1$ , b) Current and voltage of the resonant coil, c) Current of switch  $S_2$  and voltage of resonant coil

#### 4. Conclusion

In a current source parallel resonance inverter, it is desirable to operate closer to the resonant frequency for the inverter to operate in zero-voltage switching. Since both switches are connected to ground in this inverter, they are easy to drive and do not need additional driver circuit.

In a parallel resonant inverter, there are some ranges where the output voltage opposes the output current. The phase difference between the output current and voltage depends on the switching frequency. At the resonant frequency, the phases are the same. Current source parallel resonance inverters are preferred in applications that require high current and low voltage at the output.

In the circuit proposed for the simulation, the resonance frequency of the class D current fed resonance inverter is 75026.35967 Hz, the resonant coil current is 110.942 A, the resonant tank voltage is 150.977 V, MOSFETs current is 8.5 A and the output power is 400 W. By operating at the resonant frequency, switching is provided at zero voltage. Thus, switching losses are prevented and maximum efficiency is achieved.

#### REFERENCES

- [1] D. K. Cheng, "Zamanla Değişen Alanlar ve Maxwell Denklemleri," in *Mühendislik Elektromanyetiğinin Temelleri*, A. Köksal and B. Saka, Eds. Ankara: Palme Yayıncılık, 2015, p. 234.
- [2] İ. Kara, "PLC – PDM Kontrollü İndüksiyon Isıtma Sistemi," Karabük Üniversitesi, Karabük, Türkiye, 2018.
- [3] A. Polsripim, S. Chudjuarjeen, A. Sangswang, P. N. N. Ayudhya, and C. Koompai, "A Soft Switching Class D Current Source Inverter for Induction Heating with Ferromagnetic Load," *2009 Int. Conf. Power Electron. Drive Syst.*, pp. 877–881, 2009.
- [4] A. Suresh and S. R. Reddy, "Simulation of Closed Loop Controlled Current Source Inverter fed Ferromagnetic Load," pp. 161–164, 2010.
- [5] J. Jittakort, A. Sangswang, S. Naetiladdanon, C. Koompai, and S. Chudjuarjeen, "A soft switching class D current source inverter for induction heating with non-ferromagnetic load," 2011.
- [6] C. Ekkaravarodome, P. Thounthong, and K. Jirasereeamornkul, "Implementation of zero-ripple line current induction cooker using class-d current-source resonant inverter with parallel-load network parameters under large-signal excitation," *J. Electr. Eng. Technol.*, vol. 13, no. 3, pp. 1251–1264, 2018, doi: 10.5370/JEET.2018.13.3.1251.
- [7] A. T. Yapıcı and N. Abut, "İndüksiyonla Isıtma Uygulamaları için Bir Seri Rezonans İnverter Topolojisi ve Simülasyonu," *Kocaeli Üniversitesi Fen Bilim. Derg.*, vol. 1, no. 1, pp. 20–24, 2018.
- [8] S. Oncu and H. Ozbay, "Simulink model of parallel resonant inverter with DSP based PLL controller," *Elektron. ir Elektrotehnika*, vol. 21, no. 6, pp. 14–17, 2015, doi: 10.5755/j01.eee.21.6.13751.
- [9] A. Chakraborty, P. K. Sadhu, K. Bhaumik, P. Pal, and N. Pal, "Behaviour of a high frequency parallel quasi resonant inverter fitted induction heater with different switching frequencies," *Int. J. Electr. Comput. Eng.*, vol. 6, no. 2, pp. 447–457, 2016, doi: 10.11591/ijece.v6i1.8034.
- [10] S. I. Annie, K. M. Salim, Z. Tasneem, and M. R. Uddin, "Frequency analysis of a ZVS parallel quasi resonant inverter for a solar based induction heating system," *ECCE 2017 - Int. Conf. Electr. Comput. Commun. Eng.*, pp. 317–320, 2017, doi: 10.1109/ECACE.2017.7912924.
- [11] S. S. Choi, C. W. Lee, I. D. Kim, J. H. Jung, and D. H. Seo, "New Induction Heating Power Supply for Forging Applications Using IGBT Current-Source PWM Rectifier and Inverter," *ICEMS 2018 - 2018 21st Int. Conf. Electr. Mach. Syst.*, pp. 709–713, 2018, doi: 10.23919/ICEMS.2018.8549080.
- [12] M. S. Goh, S. S. Choi, and I. D. Kim, "High Power Factor Induction Heating Power Supply for Forging Applications Using 3-Phase 3-Switch PWM Current Source Rectifier," *Trans. Korean Inst. Electr. Eng.*, vol. 70, no. 4, pp. 457–466, 2021, doi: 10.5370/KIEE.2021.70.3.457.
- [13] G. Yalçın, "Üç Fazlı Gerilim Kaynaklı Tamköprü Paralel Rezonans İnvertörlü İndüksiyon Isıtma Sistemi," Marmara Üniversitesi, İstanbul, Türkiye, 2014.
- [14] S. Çetin, "Bir fazlı bir indüksiyon ısıtma sistemi analizi ve dizaynı," Pamukkale Üniversitesi, Pamukkale, Türkiye, 2005.
- [15] S. Öncü, "Bir Fazlı Yüksek Verimli Ev Tipi Bir İndüksiyon Isıtma Sistemi," Pamukkale Üniversitesi, Pamukkale, Türkiye, 2005.
- [16] H. E. Özden, "Yüksek Frekanslı İndüksiyon Isıtma Sistemi Tasarımı ve Uygulaması," Karabük Üniversitesi, Karabük, Türkiye, 2020.